

Inhibition of Bcr-Abl Phosphorylation and Induction of Apoptosis by Pyrazolo[3,4-*d*]pyrimidines in Human Leukemia Cells

Fabrizio Manetti,^[a] Annalisa Pucci,^[c] Matteo Magnani,^[a] Giada A. Locatelli,^[d] Chiara Brullo,^[b] Antonella Naldini,^[c] Silvia Schenone,^{*,[b]} Giovanni Maga,^[d] Fabio Carraro,^[c] and Maurizio Botta^{*,[a]}

*A series of pyrazolo[3,4-*d*]pyrimidines, previously found to be Src inhibitors, was tested for their ability to inhibit proliferation of three Bcr-Abl-positive human leukemia cell lines (K-562, KU-812, and MEG-01), on the basis of the experimental evidence that various Src inhibitors are also active against Bcr-Abl kinase (the so called dual Src/Abl inhibitors). They reduce Bcr-Abl tyrosine phos-*

phorylation and promote apoptosis of the Bcr-Abl-expressing cells. A cell-free enzymatic assay on isolated c-Abl confirmed that such compounds directly inhibit Abl activity. Finally, molecular modeling simulations were also performed to hypothesize the binding mode of the compounds into the Abl binding site.

Introduction

Chronic myeloid leukemia (CML) is a hematological malignancy characterized by the Bcr-Abl genetic translocation and constitutive activation of the Abl tyrosine kinase. In particular, CML is a myeloproliferative disease characterized by the balanced reciprocal translocation of c-Abl protooncogene from chromosome 9 to the break point cluster region of Bcr gene on chromosome 22, leading to the formation of the Philadelphia chromosome. In the recent past, advances in the selective inhibition of Bcr-Abl kinase activity led to the development of imatinib mesylate (Gleevec) that now represents the first-line treatment for CML. However, Bcr-Abl gene amplification that leads to overexpression of the Bcr-Abl protein, point mutations in the Bcr-Abl kinase domain that interfere with imatinib binding, and point mutations outside of the kinase domain that allosterically inhibit imatinib binding to Bcr-Abl, are all known to confer resistance to Gleevec. As a consequence, there is a growing interest in developing second-generation small molecule inhibitors able to treat Gleevec-resistant CML.^[1] For this purpose, in addition to selective inhibitors of Bcr-Abl,^[2] several classes of structurally diverse compounds appeared in recent literature, able to inhibit either kinases of the Src family or Abl kinase, because of their considerable homology (referred to as dual Src-Abl inhibitors).^[3] Based on the fact that compounds acting as Src inhibitors often also showed activity toward Bcr-Abl, we planned to test a series of pyrazolo[3,4-*d*]pyrimidine derivatives (previously found to inhibit c-Src)^[4] on a panel of three human leukemia cell lines and towards the Abl enzyme in a cell-free assay. In particular, compounds 1–7 were found to inhibit proliferation and promote apoptosis in Bcr-Abl-expressing cells, such as the CML K-562 cells, the basophilic leukemia KU-812 cell line, and the CML blastic (megakaryoblastic) MEG-01 cell line. These effects were accompanied by reduction

of cellular tyrosine phosphorylation of Bcr-Abl and one of its downstream signaling effectors (namely, the signal transducer and activator of transcription 5, STAT-5). The biochemical assay with human recombinant Abl demonstrated inhibition of Abl-catalyzed peptide substrate phosphorylation.

Results and discussion

Inhibition of proliferation. To assess the potency of compounds 1–7, their effects on three Bcr-Abl-positive leukemia cell lines were evaluated in proliferation and apoptosis assays, in comparison to (1-(*tert*-butyl)-3-(4-chlorophenyl)-4-aminopyrazolo[3,4-*d*]pyrimidine (PP2), which was used as the reference compound. Although recent literature reports several examples of compounds that could be used as comparators to validate enzymatic and cell models, PP2 was used as the reference com-

- [a] Dr. F. Manetti, Dr. M. Magnani, Prof. Dr. M. Botta
Dipartimento Farmaco Chimico Tecnologico, Università degli Studi di Siena
Via Alcide de Gasperi 2, 53100 Siena (Italy)
Fax: (+39) 0577-234333
E-mail: botta@unisi.it
- [b] Dr. C. Brullo, Prof. Dr. S. Schenone
Dipartimento di Scienze Farmaceutiche, Università degli Studi di Genova
Viale Benedetto XV 3, 16132 Genova (Italy)
Fax: (+39) 010-3538358
E-mail: schensil@unige.it
- [c] Dr. A. Pucci, Prof. Dr. A. Naldini, Prof. Dr. F. Carraro
Dipartimento di Fisiologia, Sezione di Neuroimmunofisiologia, Università degli Studi di Siena
Via Aldo Moro, 53100 Siena (Italy)
- [d] Dr. G. A. Locatelli, Dr. G. Maga
Istituto di Genetica Molecolare, IGM-CNR
Via Abbategrasso 207, 27100 Pavia (Italy)

compound for three main reasons. 1) Although initially identified as a potent and selective inhibitor of Src tyrosine kinases,^[5] PP2 also inhibits c-Abl with a similar potency.^[6] As a consequence, it is an appropriate reference compound when activity towards both Src and Abl is to be compared. 2) A huge amount of literature has been published on PP2 during the last decade, giving us exhaustive information on its biological profile toward both Src and Abl, and other kinases. 3) PP2 is an easily available commercial compound.

Results of antiproliferative assays allowed us several tentative considerations concerning the relationship between the structure and the activity of the new compounds. In particular, the decrease in the viability of K-562 cells treated with the pyrazolo-pyrimidine derivatives was assessed using the colorimetric MTT assay. Experiments performed to determine the in vitro effects of such compounds displayed a significant antiprolifera-

tive activity on K-562 cells. In fact, activity data were in the low micromolar range, spanning from 19 to 176 μM for **5i** and **1l**, respectively (Table 1). The most active compound **5i** belonged to the class of molecules bearing a styryl moiety at N1 and unsubstituted at position 6. Among them, the 4-cyclohexylamino and the 4-morpholino derivatives **5h** and **5g** also showed appreciable activity (29 and 24 μM , respectively), whereas the activity of the remaining compounds of this class was significantly lower. When a methylthio or an ethylthio group was introduced at position 6 (as in compounds **3** and **4**, respectively), activity remained in the low micromolar range. Introduction of a hydroxyphenylethyl side chain at N1 led to compounds **6** with activity ranging from 56 to 145 μM , lower than the corresponding bromo analogues **7**. Similarly, good activity values were found among compounds with a chlorophenylethyl side chain at N1 and a methylthio (**1**) and an ethylthio group (**2**) at

Table 1.

Structure and inhibitory activity of compounds 1–7 toward isolated Abl kinase and human leukemia K-562, MEG-01, and KU-812 cell lines.

Compd	R	R ¹	R ^{2(a)}	K _i [μM] ^(b)	IC ₅₀ [μM] ^(c)		
					K-562 ^(d)	MEG-01	KU-812
1a	SMe	NHPr	A	4.8 ± 0.6	28 ± 1	34 ± 2	
1b	SMe	NHBu	A	1.2 ± 0.3	29 ± 1	25 ± 3	
1c	SMe	N(Et) ₂	A	0.4 ± 0.1	31 ± 1	40 ± 2	
1d	SMe	NH(CH ₂) ₂ OEt	A	1.5 ± 0.5	34 ± 1	37 ± 1	
1e	SMe	1-pyrrolidinyl	A	NA	64 ± 1	93 ± 4	
1f	SMe	1-piperidinyl	A	NA	43 ± 1	69 ± 2	
1g	SMe	4-morpholinyl	A	NA	54 ± 1	19 ± 1	
1h	SMe	1-hexahydroazepinyl	A	5.9 ± 0.9	42 ± 1	40 ± 1	
1i	SMe	NHcyclohexyl	A	NA	39 ± 1	25 ± 2	
1j	SMe	NHBn	A	0.3 ± 0.1	34 ± 3	21 ± 1	
1k	SMe	NH(CH ₂) ₂ Ph	A	7.3 ± 1.2	30 ± 1	3.6 ± 0.7	83 ± 2
1l	SMe	4-(2,6-dimethyl)-morpholinyl	A	3.5 ± 0.7	176 ± 17	28 ± 2	
2a	SEt	NHPr	A	4.1 ± 0.4	23 ± 1	14 ± 2	73 ± 5
2b	SEt	NHBu	A	0.3 ± 0.1	27 ± 1	18 ± 1	
2c	SEt	1-pyrrolidinyl	A	NA	38 ± 1	32 ± 2	
2d	SEt	1-piperidinyl	A	NA	38 ± 1	54 ± 2	
2e	SEt	4-morpholinyl	A	NA	31 ± 1	9.4 ± 0.8	87 ± 1
2f	SEt	NHBn	A	NA	27 ± 1	15 ± 0.4	
2g	SEt	4-(2,6-dimethyl)-morpholinyl	A	11 ± 2	56 ± 2	16 ± 1	
3a	SMe	NHBn	B	1.9 ± 0.4	55 ± 1	25 ± 2	
3b	SMe	NH(CH ₂) ₂ Ph	B	0.4 ± 0.1	56 ± 1	23 ± 1	
3c	SMe	1-piperidinyl	B	1.3 ± 0.5	59 ± 1	42 ± 3	
3d	SMe	4-morpholinyl	B	6.8 ± 1.4	58 ± 1	46 ± 4	
3e	SMe	4-(2,6-dimethyl)-morpholinyl	B	4.7 ± 1.0	103 ± 2	42 ± 2	
4a	SEt	4-morpholinyl	B	9.0 ± 1.8	75 ± 2	12 ± 1	
4b	SEt	4-(2,6-dimethyl)-morpholinyl	B	6.1 ± 1.7	62 ± 1	64 ± 4	
5a	H	NHPr	B	7.4 ± 0.6	49 ± 1	32 ± 1	
5b	H	NHcyclopropyl	B	NA	69 ± 3	30 ± 1	
5c	H	NHBu	B	0.4 ± 0.1	42 ± 2	23 ± 1	
5d	H	NH(CH ₂) ₂ OEt	B	12 ± 3	39 ± 1	41 ± 2	
5e	H	1-pyrrolidinyl	B	3.9 ± 0.6	50 ± 3	48 ± 2	
5f	H	1-piperidinyl	B	0.2 ± 0.1	80 ± 2	48 ± 2	
5g	H	4-morpholinyl	B	7.8 ± 2.1	24 ± 4	25 ± 1	
5h	H	NHcyclohexyl	B	0.8 ± 0.2	29 ± 4	41 ± 6	

Table 1. (Continued)

Compd	R	R ¹	R ^{2(a)}	K _i [μM] ^[b]		IC ₅₀ [μM] ^[c]	
5i	H	hexahydroazepinyl	B	0.3 ± 0.1	19 ± 2 (30 ± 1)	51 ± 1	26 ± 1
5j	H	NHBn	B	3.8 ± 1.0	85 ± 4	82 ± 4	
5k	H	NH(CH ₂) ₂ Ph	B	9.7 ± 2.2	150 ± 15	33 ± 1	
6a	H	NHPr	C	NA	87 ± 2	55 ± 4	
6b	H	1-piperidinyl	C	NA	85 ± 1	32 ± 5	
6c	H	NHBn	C	NA	113 ± 8	44 ± 2	
6d	H	NHBu	C	NA	145 ± 2	34 ± 3	
6e	H	4-morpholinyl	C	NA	80 ± 1	91 ± 9	
6f	H	NH(CH ₂) ₂ Ph	C	NA	61 ± 1	29 ± 3	
6g	H	NHCH ₂ C ₆ H ₄ - <i>p</i> -F	C	NA	56 ± 1	59 ± 2	
7a	H	NHPr	D	4.8 ± 1.2	68 ± 1	43 ± 1	
7b	H	NHcyclopropyl	D	NA	89 ± 7	38 ± 2	
7c	H	NHPr	D	2.1 ± 0.3	94 ± 2	32 ± 1	
7d	H	NHBu	D	0.7 ± 0.1	34 ± 1 (57 ± 1)	19 ± 1	58 ± 2
7e	H	NH(CH ₂) ₂ OEt	D	1.6 ± 0.4	78 ± 1	46 ± 1	
7f	H	1-pyrrolidinyl	D	0.9 ± 0.2	57 ± 3	35 ± 1	
7g	H	1-piperidinyl	D	1.2 ± 0.5	63 ± 2	46 ± 1	
7h	H	4-morpholinyl	D	0.2 ± 0.1	69 ± 1	56 ± 2	
7i	H	NHcyclohexyl	D	0.5 ± 0.1	38 ± 1 (50 ± 1)	33 ± 1	71 ± 4
7j	H	1-hexahydroazepinyl	D	4.9 ± 1.6	44 ± 2	39 ± 1	
7k	H	NHBn	D	3.1 ± 0.4	48 ± 1	63 ± 5	
PP2				0.5 ± 0.2	75 ± 1 (25 ± 1)	17 ± 1	45 ± 3

[a] A = 2-chloro-2-phenylethyl, B = styryl, C = 2-hydroxy-2-phenylethyl, D = 2-bromo-2-phenylethyl. [b] K_i values toward isolated Abl calculated according to the following equation: $K_i = ID_{50} / \{E_0 + [E_0 \cdot (K_m(ATP)/S_0)]\} / E_0$, where E₀ and S₀ are the enzyme and the ATP concentrations (0.005 and 0.012 μM, respectively). NA = Not Active (ID₅₀ > 200 μM). ND = Not Determined. [c] IC₅₀ values are means ± SD of five experiments, each performed in triplicate. NA = not active at 100 μM. [d] In parentheses, IC₅₀ values obtained with the ATP-based assay.

position 6. In summary, a propylamino, butylamino, and arylamino (that is, benzylamino and phenylethylamino) side chains at C4 were the most profitable moieties for activity of compounds bearing a chlorophenylethyl side chain at N1, irrespective of the substituent at position 6. In contrast, cyclic groups (that is, hexahydroazepino, morpholino, and cyclohexylamino) were associated with the best activity among 6-unsubstituted styryl derivatives. Regarding bromo derivatives **7**, optimal C4 amino side chains described above were associated with good activity values. As examples, butylamino, cyclohexylamino, hexahydroazepino, and benzylamino derivatives showed activity in the range of 34 and 48 μM.

Six of the most active compounds as determined by the MTT assay (namely, **1k**, **2a**, **2e**, **5i**, **7d**, and **7i**), were also tested towards the same cell line, in a more accurate ATP-based assay (Table 1). Results indicated that the styryl derivative **5i** was the most potent compound toward K-562 cells, showing an activity comparable to that of the reference compound PP2 (30 versus 25 μM, respectively). Following a similar approach, this compound was also found as the most active toward the basophilic leukemia cells KU-812 with an activity of 26 μM, about two-fold better than that found for PP2 (45 μM).

The remaining five compounds showed activity values in the range of 58 to 87 μM.

Regarding MEG-01 cells, 6-unsubstituted-1-styryl derivatives bearing a short alkylamino (propylamino, butylamino, and cyclopropylamino for compound **5a**, **5c**, and **5b**, respectively), a morpholino (**5g**), and a phenylethylamino (**5k**) side chain at C4 were all characterized by good activity (from 23 to 33 μM, Table 1). Introduction of a methylthio group at C6 caused a twofold decrease in activity of the morpholino derivative (46 μM of **3d** versus 25 μM of **5g**), whereas aryl compounds **3a**, **b** showed better activity with respect to the corresponding 6-unsubstituted analogues **5j**, **k**. On the contrary, increasing the size of the methylthio to an ethylthio group led to a two- and fourfold increase in activity of the morpholino derivative **4a** in comparison to **5g** and **3d**, respectively. Among N1 hydroxy- and bromophenylethyl derivatives, **6f** and **7d** retained good activity (29 and 19 μM, respectively). However, a significant improvement of activity was found for compounds bearing a N1-chlorophenylethyl side chain and a 6-alkylthio substituent. In particular, morpholino and arylamino derivatives were characterized by activity values spanning from 3.6 to 19 μM, with the best activity found for the phenylethyl com-

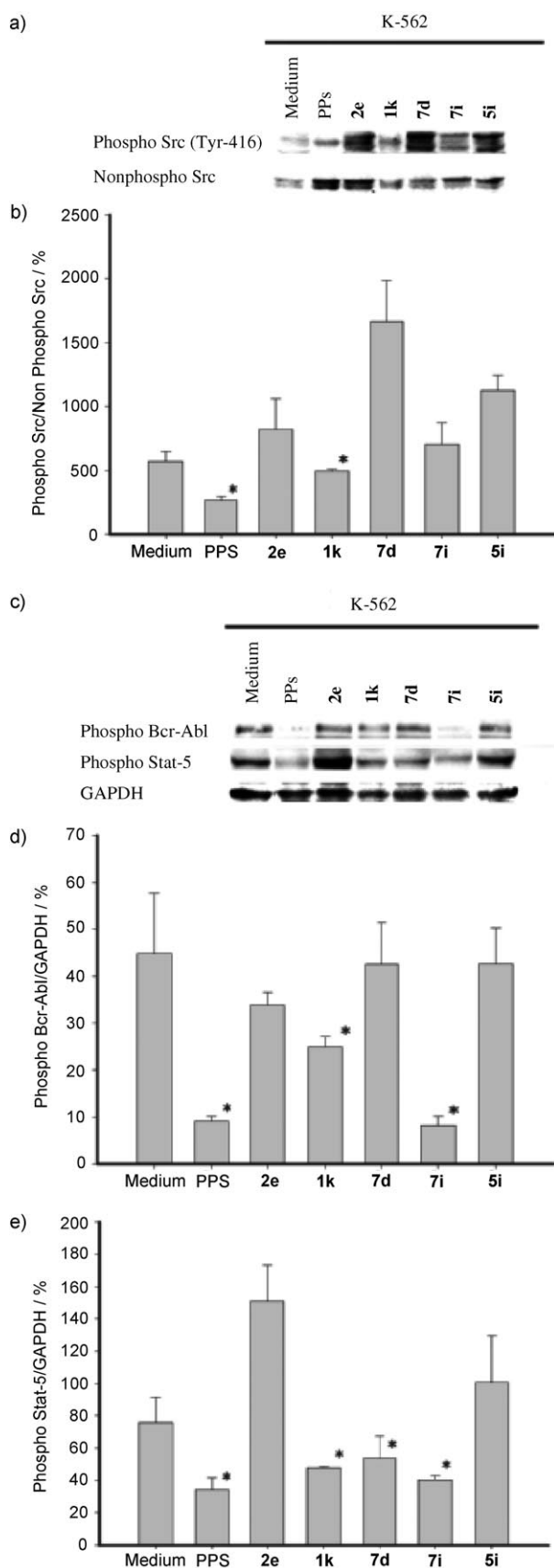


Figure 1. Effect of compounds **1k**, **2e**, **5i**, **7d**, and **7i** on the phosphorylation of Src, Bcr-Abl, and STAT-5 in K-562 cells, in comparison to the reference compound PP2. a) Lane 1: cell control; lane 2: cells challenged for 3 h in the

presence of 50 μM PP2; lane 3–7: cells challenged for 3 h in the presence of 50 μM of the test compound. After 3 h, cell lysates were obtained and analyzed. Immunoblot analysis was performed using phospho-specific antibodies to Src (Tyr 416). Filters were additionally reprobated with specific nonphospho anti-Src antibodies after stripping. b) Quantification of phospho and nonphospho Src expression was achieved with Sigma Gel analysis software and results represented the percent of the phospho Src over nonphospho Src. c) Lane 1: cell control; lane 2: cells challenged for 3 h in the presence of 50 μM PP2; lane 3–7: cells challenged for 3 h in the presence of 50 μM of the tested compound. After 3 h, cell lysates were obtained and analyzed. Immunoblot analysis was performed using a mix of phospho-specific antibodies to Bcr-Abl and STAT-5, and GAPDH as control. Quantification of phospho Bcr-Abl, phospho STAT-5, and GAPDH expression was achieved with Sigma Gel analysis software and results represented the percent of the phospho Bcr/Abl over GAPDH (d) and phospho STAT-5 over GAPDH (e). The means \pm SEM of three independent experiments are presented. Asterisks indicate statistically significant differences between control and K-562 cells treated with specific compound. Statistical analyses were performed using Student's *t* test and Bonferroni's correction.

presence of 50 μM PP2; lane 3–7: cells challenged for 3 h in the presence of 50 μM of the test compound. After 3 h, cell lysates were obtained and analyzed. Immunoblot analysis was performed using phospho-specific antibodies to Src (Tyr 416). Filters were additionally reprobated with specific nonphospho anti-Src antibodies after stripping. b) Quantification of phospho and nonphospho Src expression was achieved with Sigma Gel analysis software and results represented the percent of the phospho Src over nonphospho Src. c) Lane 1: cell control; lane 2: cells challenged for 3 h in the presence of 50 μM PP2; lane 3–7: cells challenged for 3 h in the presence of 50 μM of the tested compound. After 3 h, cell lysates were obtained and analyzed. Immunoblot analysis was performed using a mix of phospho-specific antibodies to Bcr-Abl and STAT-5, and GAPDH as control. Quantification of phospho Bcr-Abl, phospho STAT-5, and GAPDH expression was achieved with Sigma Gel analysis software and results represented the percent of the phospho Bcr/Abl over GAPDH (d) and phospho STAT-5 over GAPDH (e). The means \pm SEM of three independent experiments are presented. Asterisks indicate statistically significant differences between control and K-562 cells treated with specific compound. Statistical analyses were performed using Student's *t* test and Bonferroni's correction.

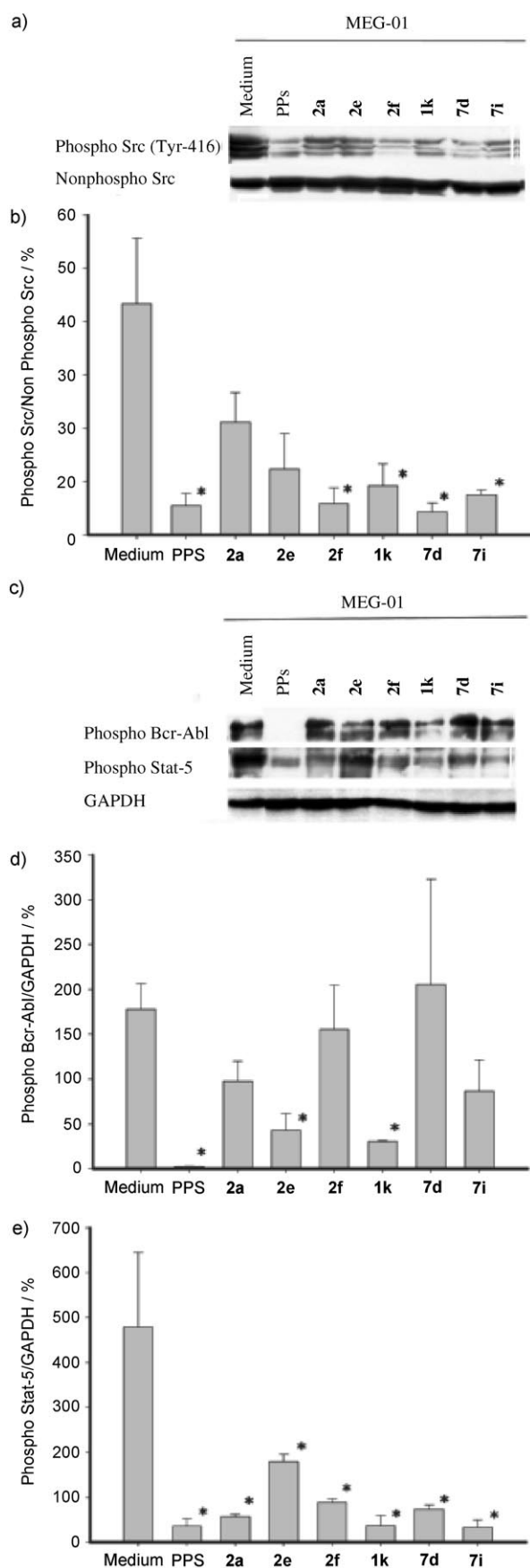
compound **1k** (3.6 μM) and for the morpholino derivative **2e** (9.4 μM), better in both cases than that of PP2 (17 μM).

Inhibition of phosphorylation of Bcr-Abl and its downstream target STAT-5. Inhibition of Src phosphorylation. With the aim of better understanding the antiproliferative activity of these new compounds toward leukemia cells, some of them were selected (on the basis of their biological profile in terms of activity toward cell lines) to be submitted to further assays. Specifically, to check in each cell line if a direct link between the antiproliferative effects of pyrazolo-pyrimidines and the inhibition of Bcr-Abl activity does exist, we evaluated the phosphorylation of both Bcr-Abl and its downstream substrate STAT-5 (Bcr-Abl is known to phosphorylate STAT-5, a transcription factor directly activating Bcl-xL, which in turn acts at the level of mitochondria to inhibit apoptosis), in addition to phosphorylation of Src. Specifically, compounds **1k**, **2e**, **5i**, **7d**, and **7i** were chosen for K-562 cells, compounds **1k**, **2a**, **2e**, **2f**, **7d**, and **7i** were chosen for MEG-01 cells, and compounds **1k**, **2a**, **2e**, **5i**, **7d**, and **7i** were chosen for KU-812 cells in addition to PP2 which is used as a reference compound. As a result, immunoblot analysis of lysates from compound-treated cells with specific antiphospho antibodies revealed a reduction in phosphorylation of all the targets. Taken together, reduction of phosphorylation levels of both Bcr-Abl and STAT-5 strongly suggested that effects mediated by compounds on proliferation and apoptosis (see below) of leukemia cells are a consequence of the reduction of Bcr-Abl kinase activity.

Regarding K-562 cells, **1k** showed a significant inhibition of Src phosphorylation, but lower than that found for the reference compound PP2 (Figure 1 a and b). On the other hand, **7i** strongly inhibited Bcr-Abl phosphorylation, with an activity comparable to that of PP2 (Figure 1 c and d), whereas **1k**, **7d**, and **7i** reduced STAT-5 phosphorylation to a slightly lower extent than PP2 (Figure 1 c and e).

Compounds **2f** and **7d** showed an inhibitory activity on the Src phosphorylation of MEG-01 similar to that of PP2, whereas **1k** and **7i** retained activity somewhat (Figure 2 a and b). Bcr-Abl phosphorylation was significantly reduced by **2e** and **1k** (to a lower extent if compared with PP2, Figure 2 c and d), whereas STAT-5 phosphorylation was inhibited by **2a**, **1k**, and

presence of 50 μM PP2; lane 3–7: cells challenged for 3 h in the presence of 50 μM of the test compound. After 3 h, cell lysates were obtained and analyzed. Immunoblot analysis was performed using phospho-specific antibodies to Src (Tyr 416). Filters were additionally reprobated with specific nonphospho anti-Src antibodies after stripping. b) Quantification of phospho and nonphospho Src expression was achieved with Sigma Gel analysis software and results represented the percent of the phospho Src over nonphospho Src. c) Lane 1: cell control; lane 2: cells challenged for 3 h in the presence of 50 μM PP2; lane 3–7: cells challenged for 3 h in the presence of 50 μM of the tested compound. After 3 h, cell lysates were obtained and analyzed. Immunoblot analysis was performed using a mix of phospho-specific antibodies to Bcr-Abl and STAT-5, and GAPDH as control. Quantification of phospho Bcr-Abl, phospho STAT-5, and GAPDH expression was achieved with Sigma Gel analysis software and results represented the percent of the phospho Bcr/Abl over GAPDH (d) and phospho STAT-5 over GAPDH (e). The means \pm SEM of three independent experiments are presented. Asterisks indicate statistically significant differences between control and K-562 cells treated with specific compound. Statistical analyses were performed using Student's *t* test and Bonferroni's correction.



7i (with activity comparable to PP2, Figure 2c and e). Compounds **7d** and **2f** showed reduced activity toward STAT-5, in comparison to that of PP2.

Finally, Src phosphorylation of KU-812 cells was markedly affected by **2a** with an activity higher than that of PP2 (Figure 3a and b). Compounds **1k**, **7d**, **7i**, and **2a** were able to inhibit Bcr-Abl phosphorylation with an activity comparable to PP2 (Figure 3c and d), whereas **7d** and **7i** (**2a** and **2e** with reduced extension) interfered with STAT-5 phosphorylation (Figure 3c and e).

Proapoptotic activity: PARP assay and studies on Bax/Bcl-xL expression. For each cell line, the same compounds tested for their activity toward Src, Abl, and STAT-5 phosphorylation, were also evaluated for their proapoptotic activity on a Poly-ADP-Ribose-Polymerase (PARP) assay. Compounds **2e** and **5i**, as well as PP2, potentially induced apoptosis in K-562 cells (Figure 4a and b), whereas **1k**, **7d**, and **7i** showed lower proapoptotic activity, but significantly higher than that found in the control. As far as the MEG-01 cell line was concerned, the cleaved/uncleaved PARP ratio of the control was comparable to that of PP2 (Figure 4c and d), whereas proapoptotic activity of all the tested inhibitors was comparable to each other and significantly higher with respect to both control and PP2. The sole exception was represented by **2f** with insignificant proapoptotic activity. Analysis of the proapoptotic activity toward KU-812 cells showed that **7i** induced apoptosis better than **2e** and **7d** (with activity comparable to the control), whereas the remaining compounds (including PP2) were characterized by significantly lower proapoptotic activity (Figure 4e and f).

Finally, on the basis of the ability of some of these compounds to induce apoptosis in both cell lines, we also investigated the expression of Bax/Bcl-xL mRNA in KU-812. It is known that molecular mechanisms of apoptosis, in addition to causing release of cytochrome C from mitochondria to the cytosol, involve changes in the expression of distinct genes. As an example, the ratio of proapoptotic Bax and antiapoptotic Bcl-2 or Bcl-xL genes appears to be a critical determinant to

Figure 2. Effect of compounds **1k**, **2a**, **2e**, **2f**, **7d**, and **7i** on the phosphorylation of Src, Bcr-Abl, and STAT-5 in MEG-01 cells, in comparison to the reference compound PP2. a) Lane 1: cell control; lane 2: cells challenged for 3 h in the presence of 50 μM PP2; lane 3–8: cells challenged for 3 h in the presence of 50 μM of the test compound. After 3 h, cell lysates were obtained and analyzed. Immunoblot analysis was performed using phospho-specific antibodies to Src (Tyr416). Filters were additionally reprobbed with specific nonphospho anti-Src antibodies after stripping. b) Quantification of phospho and nonphospho Src expression was achieved with Sigma Gel analysis software and results represented the percent of the phospho Src over nonphospho Src. c) Lane 1: cell control; lane 2: cells challenged for 3 h in the presence of 50 μM PP2; lane 3–8: cells challenged for 3 h in the presence of 50 μM of the test compound. After 3 h, cell lysates were obtained and analyzed. Immunoblot analysis was performed using a mix of phospho-specific antibodies to Bcr-Abl and STAT-5, and GAPDH as control. Quantification of phospho Bcr-Abl, phospho STAT-5, and GAPDH expression was achieved with Sigma Gel analysis software and results represented the percent of the phospho Bcr/Abl over GAPDH (d) and phospho STAT-5 over GAPDH (e). The means \pm SEM of three independent experiments are presented. Asterisks indicate statistically significant differences between control and MEG-01 cells treated with specific compound. Statistical analyses were performed using Student's *t* test and Bonferroni's correction.

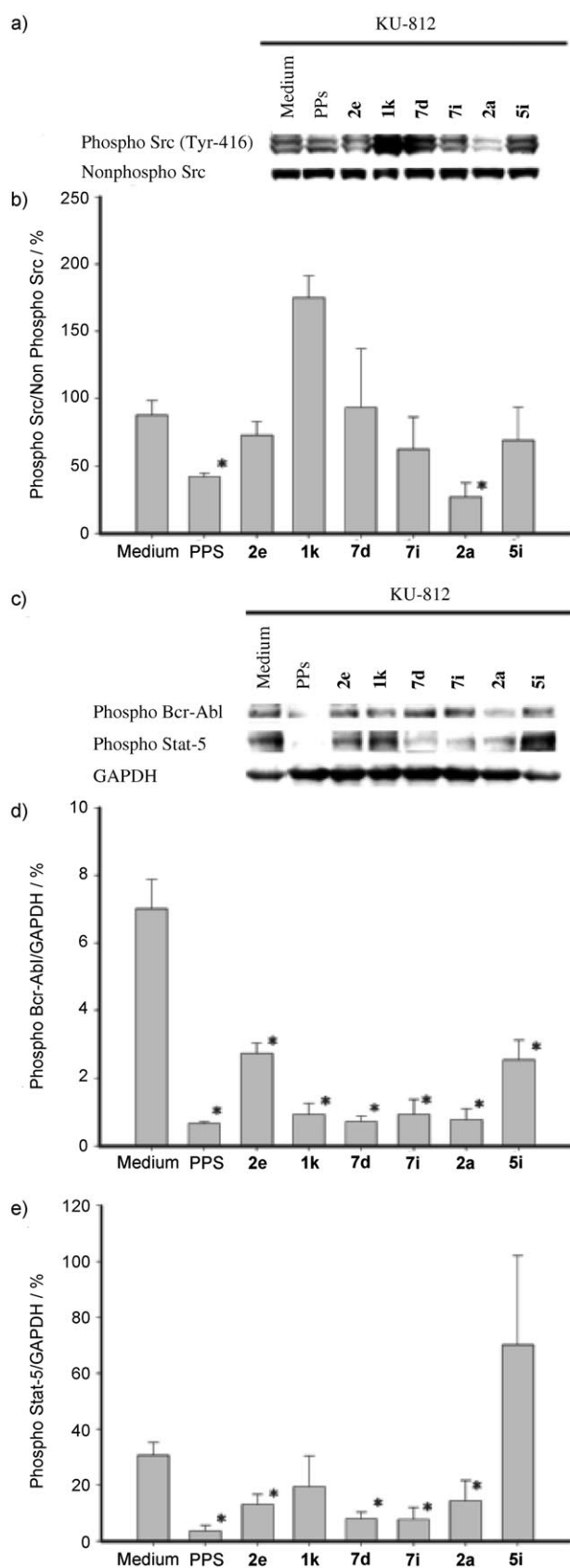


Figure 3. Effect of compounds **1k**, **2a**, **2e**, **5i**, **7d**, and **7i** on the phosphorylation of Src, Bcr-Abl, and STAT-5 in KU-812 cells, in comparison to the reference compound PP2. a) Lane 1: cell control; lane 2: cells challenged for 3 h in the presence of 50 μM PP2; lane 3–8: cells challenged for 3 h in the pres-

ence of 50 μM of the test compound. After 3 h, cell lysates were obtained and analyzed. Immunoblot analysis was performed using phospho-specific antibodies to Src (Tyr416). Filters were additionally reprobated with specific nonphospho anti-Src antibodies after stripping. b) Quantification of phospho and nonphospho Src expression was achieved with Sigma Gel analysis software and results represented the percent of the phospho Src over nonphospho Src. c) Lane 1: cell control; lane 2: cells challenged for 3 h in the presence of 50 μM PP2; lane 3–8: cells challenged for 3 h in the presence of 50 μM of the test compound. After 3 h, cell lysates were obtained and analyzed. Immunoblot analysis was performed using a mix of phospho-specific antibodies to Bcr-Abl and STAT-5, and GAPDH as control. Quantification of phospho Bcr-Abl, phospho STAT-5, and GAPDH expression was achieved with Sigma Gel analysis software and results represented the percent of the phospho Bcr/Abl over GAPDH (d) and phospho STAT-5 over GAPDH (e). The means \pm SEM of three independent experiments are presented. Asterisks indicate statistically significant differences between control and KU-812 cells treated with specific compound. Statistical analyses were performed using Student's *t* test and Bonferroni's correction.

induce cells toward apoptosis.^[7] Death signals induce an increase in expression of the Bax mRNA message, leading Bax itself to gain proapoptotic activity.^[8] On the other hand, the proapoptotic action of Bax is antagonized by Bcl-2 and Bcl-xL, which are both able to inhibit the release of cytochrome C from mitochondria. In this context, Bcr-Abl participates in maintenance of an antiapoptotic environment through the regulation of Bcl-2 antiapoptotic members.^[8d] Moreover, overexpression of Bcl-xL or Bcl-2 preserves Bax in an inactive conformation.^[8a] For the above reasons, the ratio between Bax mRNA and Bcl-xL mRNA expression may be used as a direct index of the induction of the apoptotic process and could help in explaining the molecular mechanism of apoptosis induction. As a result, incubation of KU-812 cells for 72 h in the presence of the inhibitors led to an increase in the Bax/Bcl-xL ratio (Figure 5), thus inducing apoptosis in leukemia cells.

Compounds inhibit peptide substrate phosphorylation by Abl. To examine whether the effects observed with leukemic cells were directly attributable to inhibition of Abl kinase activity, the mechanism of kinase inhibition was investigated using a cell-free assay with recombinant Abl. Results showed that many of the studied pyrazolo-pyrimidines were characterized by inhibitory activity toward Abl in the micro- and submicro-

molar range (Table 1). Moreover, an analysis of enzymatic data suggested several tentative SAR considerations. In particular, among compounds **1**, acyclic amino moieties at C4 are preferred with respect to the cyclic counterparts. As examples, the diethylamino derivative **1c** showed better activity (0.4 μM) than both the pyrrolidinyl and the piperidinyl analogues **1e** and **1f** (not active at the test dose), and the ethoxyethylamino compound **1d** was more active than the morpholino analogue **1g** (1.5 μM versus NA, respectively). This was probably due to the fact that acyclic compounds are characterized by a higher conformational mobility that allowed for a better fit into the binding site. Following this rationale, **1h**, which is more flexible than both **1f** and **1e**, showed some activity toward the enzyme (5.9 μM). Aromatic substituents at C4, as found in **1j** and **1k**, were also profitable for enzymatic inhibition.

Increasing the size of the substituent at C6 from a thiomethyl to a thioethyl group, was detrimental for enzyme inhibition. In fact, all the compounds **2** were found inactive at the test

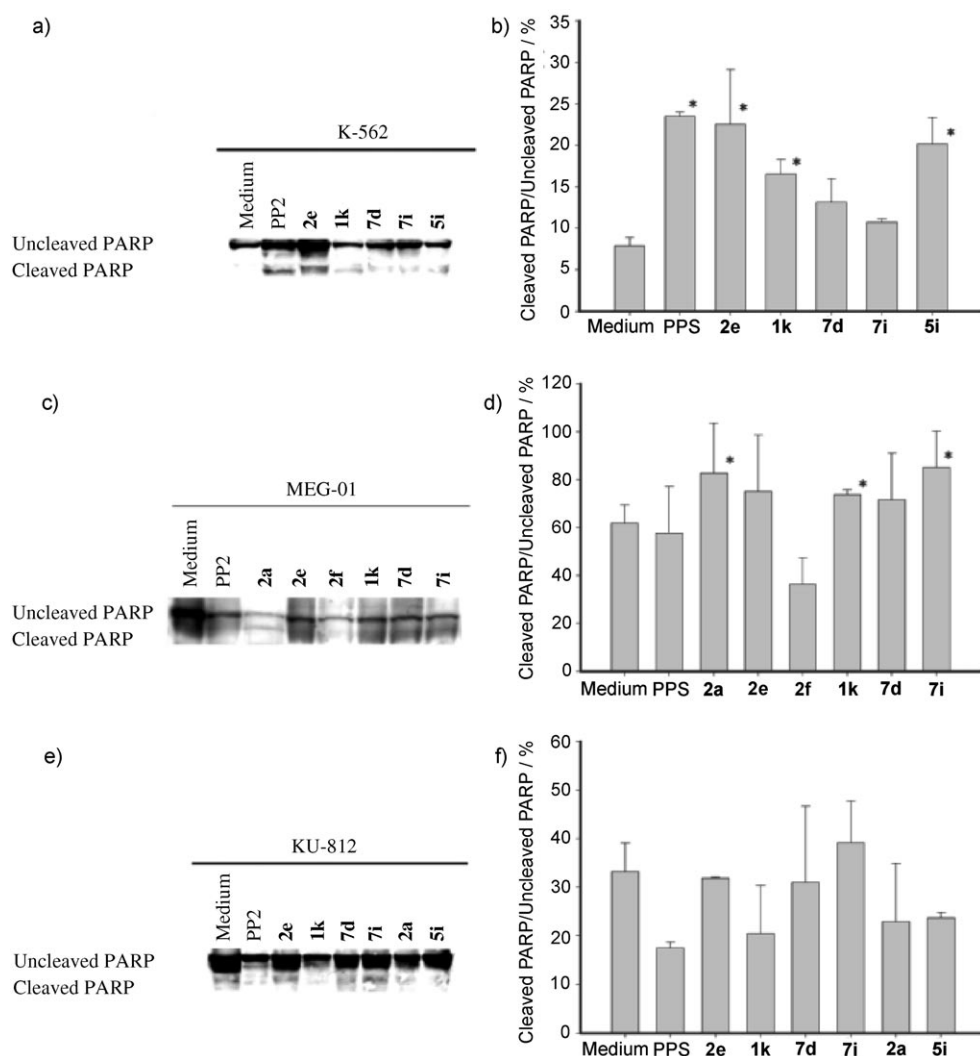


Figure 4. Proapoptotic effect of selected pyrazolo[3,4-*d*]pyrimidines on K-562 (a, b), MEG-01 (c, d), and KU-812 cells (e, f) measured by PARP cleavage, in comparison to the reference compound PP2. Cells were cultured at a concentration of 2×10^5 cells mL⁻¹. For each gel (namely, a, c, and e): lane 1: cell control; lane 2: cells challenged for 72 h with 50 μ M PP2; remaining lanes: cells challenged for 72 h in the presence of 50 μ M of the test compound. After 72 h, cell lysates were obtained and analyzed. Immunoblot analysis was performed using PARP-specific antibodies to both the uncleaved (113 kDa) and cleaved (89 kDa) forms of PARP. Quantification of PARP expression was achieved with Sigma Gel analysis software and the results, representing the percent of cleaved over uncleaved PARP, are expressed as means \pm SEM of three independent experiments (b for K-562, d for MEG-01, and f for KU-812). Asterisks indicate statistically significant differences ($p < 0.05$) between control and K-562 cells treated with the test compound. Statistical analyses were performed using Student's *t* test and Bonferroni's correction.

dose, with the exception of **2a** and **2b** (3.1 and 0.3 μ M, respectively).

Changing the N1 side chain of compounds **1** to a styryl moiety, compounds with cyclic amines at C4 acquired good activity, whereas aromatic amines (as in **3a** and **3b**) led to inhibition comparable to that of the corresponding N1 chlorophenylethyl analogues **1j** and **1k**. Compounds **4a** and **4b** showed a micromolar activity very similar to that of the methylthio compounds **3d** and **3e**.

Compounds **5**, unsubstituted at the position 6, were characterized by enzymatic inhibition similar to the corresponding methyl- and ethylthio derivatives **3** and **4**.

Introduction of a N1 bromophenylethyl side chain instead of the styryl moiety did not change the activity toward the enzyme significantly. In fact, compounds **7** showed activity values comparable to those of the corresponding styryl analogues **5**. In contrast, the hydroxyphenylethyl side chain of compounds **6** markedly influenced their inhibitory properties, making these compounds inactive at the test dose.

In summary, both cellular and biochemical assays were performed to assess the activity of pyrazolo-pyrimidine derivatives. The compounds inhibited cell proliferation and induced apoptosis of Bcr-Abl-positive leukemia cells, and reduced phosphorylation of both Bcr-Abl and a downstream Bcr-Abl target (STAT-5), suggesting that cell death was correlated to the inhibition of Bcr-Abl tyrosine kinase activity and that the inhibitor entered cells efficiently. Moreover, several compounds (namely, **1j**, **2b**, **3b**, **5i**, and **7d**) were characterized by a biological profile comparable to or better than, that found for the reference compound PP2. In fact, they showed a submicromolar inhibitory activity toward the isolated enzyme and a significant antiproliferative activity toward the three leukemia cell lines under investigation. However, it is worth noting that biological data revealed some contradictions between cellular and enzymatic assays. In fact, where-

as essentially all the compounds were active in the cellular assays within a relatively narrow range, their activity against Bcr-Abl kinase varied widely. There are, at least, three possible explanations. The first one relates to the artificial conditions of the enzymatic assay. In our *in vitro* system, we used an artificial substrate, namely a short peptide. It is possible, then, that the catalytic efficiency, and the conformation of the enzyme were abnormal under our *in vitro* conditions with respect to the physiological context of an intact cell. This is likely reflected by the rather low affinity ($K_m = 1.5 \mu$ M) displayed by the recombinant enzyme for the substrate and could also influence the affinity of the enzyme for our inhibitors. Another possible ex-

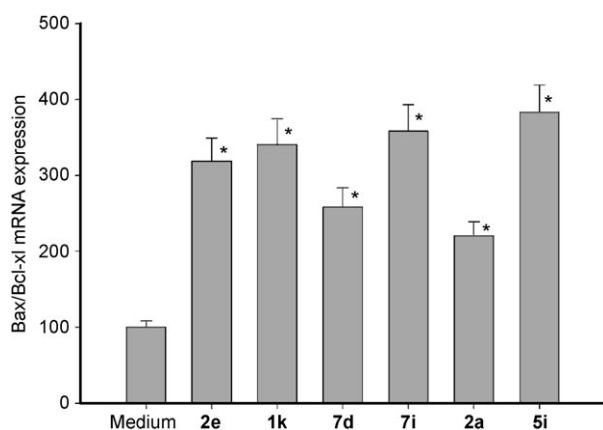


Figure 5. Effects of selected pyrazolo-pyrimidines on the expression of BAX (proapoptotic gene) and Bcl-xL (antiapoptotic gene) in KU-812 cells. Cells were cultured at a concentration of 2×10^5 cells mL^{-1} in the absence and presence of $50 \mu\text{M}$ of the test compound for 72 h at 37°C . Cell lysates from control and from cells treated with selected compounds were obtained and analyzed by qRT-PCR analysis. β -Actin was used as a housekeeping gene. Quantification of the ratio of Bax/Bcl-xL expression is reported as the mean \pm SEM of three independent experiments. The statistical analyses were performed using Student's *t* test and Bonferroni's correction.

planation for the higher activities detected in cell-based assays is that our compounds also target other kinases, such as Src toward which many of compounds 1–7 showed inhibitory activity in the micro- and submicromolar range.^[4] Moreover, preliminary experiments showed that several of the new compounds are somewhat characterized by activity against other nonreceptors or cytoplasmic tyrosine kinases, and demonstrated antiproliferative properties toward malignant cells expressing Her-2, Fak, and Akt (not shown). On the other hand, it is also possible that upon penetration into the cells, several events may occur such as an increase in drug efflux by activating the expression of the MDR1 gene, which encodes for the protein P-glycoprotein (ABCB1).^[9] Nevertheless, we are still unable to rule out if such compounds could act through a mixed-mode of Abl-Src inhibition alone or interact with additional receptors.

Molecular modeling simulations. Computational studies have been also performed to analyze the binding mode of ligands described in this work, with the aim of getting insight on the main chemical features accounting for their affinity toward the Abl enzyme. For this purpose, the three-dimensional crystal structure of the kinase domain of c-Abl in complex with the small molecule inhibitor PD173955 (entry 1M52 of the Brookhaven Protein Data Bank)^[10] was employed. The reliability of the computational protocol was preliminarily assessed by simulating the orientation of PD173955 within the ATP binding site of Abl and comparing the resulting model with the experimental data. After removal of the ligand, the structure of Abl (whose activation loop resembles that of an active kinase) was relaxed through an energy minimization routine to avoid steric bumps which may affect the X-ray structure. Next, the software Gold^[11–13] was used to carry out docking simulations of PD173955 onto the relaxed protein structure. The best ranking solution provided by the program was selected, that showed a

very good agreement with experimental data. In fact, the predicted orientation and conformation of the inhibitor was very similar to that found in the crystal structure and all of the main hydrophobic and hydrogen bond interactions characterizing the binding of PD173955 were reproduced. As the computational procedure was well able to reproduce the behavior of PD173955, it was applied to explore the interactions of the pyrazolo-pyrimidine derivatives with the kinase domain of Abl. Two different binding modes were identified, depending on the presence or absence of the alkylthio substituent at the C6 position of the pyrazolo-pyrimidine scaffold. Compounds bearing such a substituent showed an interaction pathway characterized by the pyrazolo-pyrimidine nucleus located in the region usually occupied by the adenine ring of ATP (adenine region), and by a hydrogen bond with Met318, and by several hydrophobic contacts (Figure 6a). In particular, the amino group at C4 was the hydrogen bond donor toward the carbonyl oxygen of Met318, whereas the side chains at N1 and C4 of the inhibitors were accommodated within two distinct hydrophobic regions located at opposite sides of the heterocyclic ring. The side chain at N1 interacted (van der Waals contacts) with residues Val256, Lys271, Met290, Val299, and Ile313 (constituting a large portion of the hydrophobic region I). On the

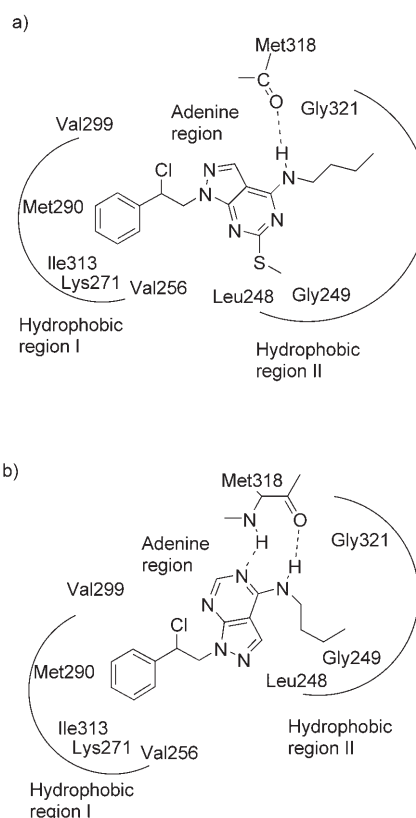


Figure 6. Schematic representation of the binding mode of the pyrazolo-pyrimidine derivatives into the ATP binding site of Abl. For the sake of clarity, only a few residues are displayed. a) Binding mode of **1b** interacting with the backbone carbonyl group of Met318 through a hydrogen bond involving the C4 amino group of the inhibitor. b) Binding mode of **7d**, engaged in two hydrogen bonds with the backbone amino and carbonyl groups of Met318. Hydrogen bonds are represented by black dashed lines.

other hand, the side chain at C4 established hydrophobic interactions with residues Leu248, Gly249, and Gly321 (constituting the hydrophobic region II). The alkylthio substituent shared the hydrophobic region II with the side chain at C4 and had van der Waals contact with residues Leu248, Gly249, and Tyr253. For compounds bearing a bulky substituent (that is, benzylamino or phenylethylamino groups) at C4, the simultaneous location of such a group and the alkylthio chain within the hydrophobic pocket II was not permitted. As a consequence, the heterocyclic nucleus was involved in a rearrangement, which resulted in the accommodation of substituents at C4 and C6 in hydrophobic region I, whereas the N1 side chain was located in hydrophobic region II. Moreover, a hydrogen bond involving the N2 of the pyrazolo-pyrimidine scaffold and the NH backbone of Met318 was found in such an orientation.

In the alternative binding mode (Figure 6b), the lack of the alkylthio substituent at the C6 position (such as **7d**) induced a reorientation of the pyrazolo-pyrimidine nucleus, without changing the location of C4 (which shares the same region as the thiomethylphenyl moiety of PD173955) and N1 (occupying a position similar to that of the dichlorophenyl ring of PD173955) side chains that were located into the hydrophobic region II and hydrophobic region I, respectively. In particular, the amino group at C4 was the hydrogen bond donor toward the carbonyl oxygen of Met318, whereas the N5 accepted a hydrogen bond from the amide NH group of the same residue (this additional hydrogen bond, with respect to the orientation reported in Figure 6a, was however not associated with a significant increase in activity, as shown in Table 1). Such a hydrogen bond pattern closely resembled that of PD173955, but differed from that of ATP (although ATP was also engaged in a pair of hydrogen bonds, its amino group interacted with the backbone carbonyl of Glu316 instead of the Met318 carbonyl group).

Finally, it is worth noting that all compounds bearing a tertiary amino group at position 4 were located with a common orientation into the binding site, independently from the presence of a substituent at the position 6. Such an orientation was very similar to that observed for compounds unsubstituted at position 6, with the C4 and N1 substituents directed toward the hydrophobic regions II and I, respectively. However, because of the absence of a hydrogen bond donor group, together with the steric hindrance occurring near the C4, the pyrazolo-pyrimidine nucleus was shifted away from Met318, resulting in the loss of the hydrogen bonds previously described, without forming any new hydrogen bond contact. Despite the absence of hydrogen bonds, many compounds with a tertiary amino group at C4 maintained an inhibitory activity comparable to that of compounds bearing a secondary amino group (thus able to establish one or two hydrogen bonds with the target).

Taken together, these results highlight the importance of hydrophobic interactions for the binding of the pyrazolo-pyrimidines to Abl kinase. In fact, even if different binding modes were identified, a full occupancy of hydrophobic regions I and II emerged as a feature common to all the active compounds. In this context, the lack of affinity affecting compounds bear-

ing a hydroxyphenylethyl side chain at N1 could be explained in terms of ineffective interactions with the hydrophobic region I, mainly due to the location of the hydrophilic hydroxy group within this region. On the other hand, hydrogen bond interactions did not seem to play a fundamental role for the affinity of compounds, in agreement with the fact that not only compounds establishing a single hydrogen bond with the target, but also many of those whose binding was characterized by no hydrogen bond, showed good inhibitory activity.

It should be also emphasized that results of docking studies on Abl kinase show some interesting similarities with results previously reported by us for the same set of compounds docked into Src kinase.^[4] In fact, in both cases, two different binding modes were identified, depending on the presence or absence of the substituent at C6. In addition, hydrogen bond interactions did not appear essential for the activity of the inhibitors toward Src.

Conclusions

The inhibition properties toward Abl in a cell-free assay, and the antiproliferative activity of some pyrazolo[3,4-*d*]pyrimidine derivatives toward a panel of human leukemia cell lines, are reported, demonstrating that several compounds are more active than PP2 (chosen as the reference compound). In particular, the studied compounds are able to inhibit Bcr-Abl and Src phosphorylation, induce apoptosis, and reduce cell proliferation as the activation of Src and Abl is an important step in the progression of leukemia cells (in particular, CML). Although the mechanism of action of such compounds at the molecular level is not yet fully understood, biological data reported herein make several of the new compounds important hits in the field of antileukemia agents, because they affect a pathway that is pivotal for the growth of transformed cells. In particular, such compounds show an important *in vitro* activity toward both Src and Abl (suggesting that some of them could be effective agents in the chemotherapy armamentarium against CML to which the so-called dual Src-Abl inhibitors were recently added), even if we can not exclude that their antiproliferative activity could in part derive from targeting other tyrosine kinases. In this context, further experiments are ongoing to check if compounds are able to affect alternative signaling pathways involved in the proliferation of leukemia cell lines.

Experimental Section

Biology

PP2 (AG 1879, 4-Amino-5-(4-chlorophenyl)-7-(*tert*-butyl)pyrazolo[3,4-*d*]pyrimidine), used as the reference compound, was purchased from Calbiochem (San Diego, CA).

Enzymatic assay on isolated Abl. The mechanism of kinase inhibition was investigated using a cell-free assay with recombinant Abl, as previously reported.^[3a] Recombinant human Abl was purchased from Upstate Biotechnology (Waltham, MA). Activity was measured in a filter-binding assay using an Abl specific peptide substrate (Abltide, Upstate Biotechnology). Reaction conditions were: 0.012 μM [γ -³²P]ATP, 50 μM peptide, 0.005 μM c-Abl. The apparent affinity (K_m) values of the Abl preparation used for its peptide and

ATP substrates were determined separately and found to be 1.5 μM and 10 μM , respectively. Kinetic analysis was performed as described elsewhere.^[3a] Each experiment was done in triplicate and mean values were used for the interpolation. Curve fitting was performed with the program GraphPad Prism.

Cell culture. Human CML K-562 cells in blast crisis,^[14] human CML MEG-01 cell line in megakaryocytic blast crisis,^[15] and human CML KU-812^[16] cell line in myeloid blast crisis were obtained from the American Type Culture Collection and were grown in RPMI 1640 medium (BioWhittaker, Vallengbaek, DK) containing 10% fetal calf serum (FCS). The cultures were free of mycoplasma. For the proliferation assay, cell lines (2×10^4 cells mL^{-1}) were incubated overnight in 100 μL RPMI 1640 culture medium (BioWhittaker), supplemented with 0.5% FCS (BioWhittaker) and antibiotics (100 U mL^{-1} penicillin and 100 $\mu\text{g mL}^{-1}$ streptomycin), at 37 °C in 5% CO_2 . Later, the spent medium was removed and the cultures were refreshed with new medium (100 μL RPMI 1640 with 10% FCS) or medium containing different concentrations (0–100 μM) of the studied compounds. After 3 days (control cultures did not reach confluence), the antiproliferative effect of the compounds was determined by 3-(4,5-dimethylthiazol-2-yl)-2,5-diphenyl-tetrazolium bromide (MTT) proliferation assay. Briefly, cells were treated with a MTT solution (10 μL , 5 mg mL^{-1}) and, four hours later, acid propan-2-ol (100 μL , 0.04 M HCl in propan-2-ol) was added to dissolve the formazan product. The microplates were read using an ELISA plate reader at 570 nm with a reference wavelength of 630 nm. Evaluation of the antiproliferative effect of some compounds on K-562 and KU-812 cell proliferation was performed by ATP lite 1 step assay (Perkin-Elmer, Boston, MA). K-562 and KU-812 cells were plated and treated with different concentration (0–150 μM) of the studied compounds, as described above. After 3 days, cells were treated with 100 μL of luciferase and D-luciferin. The plates were placed in the dark for 10 min and the luminescence was measured in a fluorescence microplate reader (FLUOstar Optima, BMG Labtech, Offenburg, Germany). Data analysis for IC_{50} calculations was performed with the LSW Data Analysis Package plug-in for Excel (Microsoft). Results are reported as mean \pm SD of five experiments, each performed in triplicate.

Western blot analysis. The inhibitory effect of compounds toward the phosphorylation of Src (Tyr416) were assessed using immunoblot analysis. Cell lines were cultured at a concentration of 2×10^5 cells mL^{-1} and challenged with the compounds (50 μM) for 3 h. Later, cells were harvested and lysed in an appropriate buffer containing 1% Triton X-100. Proteins were quantitated by the BCA method (Pierce, Rockford, IL). Equal amounts of total cellular protein were resolved by SDS-polyacrylamide gel electrophoresis, transferred to nitrocellulose filters, and subjected to immunoblot using phospho-specific antibodies against Src (Y416) (Cell Signaling Technology, Beverly, MA). Filters were additionally reprobed with specific nonphospho anti-Src antibodies (Cell Signaling Technology) after stripping. Quantification of phospho and nonphospho Src expression was achieved with Sigma Gel analysis software and results represented the percent value of the phospho Src over nonphospho Src.

The inhibitory effect of compounds toward the phosphorylation of Bcr-Abl and STAT-5 were also tested, using a PathScan Multiplex Western Detection Kit (Cell Signaling Technology). This kit was used to assay the inhibition of multiple proteins on one membrane without stripping and reprobing. Cell lines were cultured at a concentration of 2×10^5 cells mL^{-1} and challenged with the compounds (50 μM) for 3 h. Later, cells were harvested and lysed as reported above.

The proapoptotic activity of some of the compounds was also tested, using a Poly-ADP-Ribose-Polymerase (PARP) assay (Roche

Diagnostics, Milan, Italy). Cell lines were cultured at a concentration of 2×10^5 cells mL^{-1} and challenged with the compounds (50 μM). 72 h later, cells were harvested and lysed as reported above. Immunoblot analysis was performed using PARP-specific antibodies to both the uncleaved (113 kDa) and cleaved (89 kDa) forms of PARP. Quantification of phospho over nonphospho Src, phospho Bcr/Abl over GAPDH, phospho STAT-5 over GAPDH, and cleaved PARP over uncleaved PARP expression was achieved with Sigma Gel analysis software and the results, representing the percent of phospho protein over control, were expressed as the mean of three independent experiments. Statistical analyses were performed using Student's t test and the Bonferroni's correction.

mRNA Expression of apoptotic genes. The mRNA expression of apoptotic genes were performed using qRT-PCR. KU-812 cells were treated as reported above but the cells were challenged with the compounds (50 μM) for 72 h for apoptotic gene expression. Later, the cells were harvested and lysed in an appropriate buffer (OMNIZOL for RNA-DNA-Protein Extraction Kit, Euroclone, Devon, UK). The extract was processed for the extraction of mRNA. For qRT-PCR analysis, Bcl-xL (antiapoptotic gene), and bax (proapoptotic gene) expression in KU-812 cells was determined using a MJ MiniOpticon Cyclor (Bio-Rad Laboratories, Hercules, CA). First-strand cDNA synthesis was performed using iScript cDNA Synthesis Kit (Bio-Rad Laboratories). qRT-PCR was performed using iTaq SYBR Green Supermix with ROX (Bio-Rad Laboratories) and specific primers from GenBank. Data were quantitatively analyzed on an MJ Opticon Monitor detection system (Bio-Rad Laboratories). All values were expressed as fold increase relative to the expression of β -actin.

Computational details

Structures of inhibitors were represented using MacroModel 8.5^[17] and minimized with the Amber force field using the Polak-Ribiere conjugated gradient method (0.001 $\text{kJ mol}^{-1} \text{\AA}$ convergence or 10000 iterations).

To remove unfavorable contacts, a preliminary structure optimization was performed with MacroModel 8.5 on the X-ray crystallographic structure of c-Abl (entry 1M52 on the Brookhaven Protein Data Bank, 2.6 \AA resolution)^[10] through the all-atom Amber* force field and Polak-Ribiere conjugate gradient method. A continuum solvation method, with water as the solvent, was also applied. Extended cutoffs were used and convergence was set to 0.01 $\text{kJ mol}^{-1} \text{\AA}$.

Docking studies were performed by means of software Gold, version 3.0.1,^[11–13] which uses a genetic algorithm (GA) to explore the conformation/orientation space. For each of the 50 independent GA runs, a maximum number of 100000 GA operations were performed on a set of five groups with a population size of 200 individuals. The remaining GA parameters were kept to their default values. Hydrophobic fitting points were calculated on the target for a 10 \AA radius around the co-crystallized ligand PD173955. For each inhibitor, the first ranked solution was selected for further analysis.

Acknowledgements

Financial support provided by the Italian MIUR (PRIN 2004059221) and by the Fondazione Monte dei Paschi di Siena is gratefully acknowledged. We thank Dr. Giovanni Gaviraghi (Sienabiotech S.p.A.) for helpful discussion. The "Centro Universitario per l'Informatica e la Telematica" of the University of Siena is also acknowledged.

Keywords: drug design · dual Src/Abl inhibitors · leukemia cell inhibitors · medicinal chemistry · pyrazolo[3,4-d]pyrimidines

- [1] a) T. Tauchi, K. Ohyashiki, *Int. J. Hematol.* **2006**, *83*, 294–300; b) M. Buschbeck, *Drugs R&D* **2006**, *7*, 73–86; c) J. Cortes, *Curr. Opin. Hematol.* **2006**, *13*, 79–86; d) T. O'Hare, A. S. Corbin, B. J. Druker, *Curr. Opin. Genet. Dev.* **2006**, *16*, 92–99; e) T. O'Hare, D. K. Walters, E. P. Stoffregen, D. W. Sherbenou, M. C. Heinrich, M. W. Deininger, B. J. Druker, *Clin. Cancer Res.* **2005**, *11*, 6987–6993; f) C. Walz, M. Sattler, *Crit. Rev. Oncol. Hematol.* **2006**, *57*, 145–164; g) M. Azam, G. Q. Daley, *Mol. Diagn. Ther.* **2006**, *10*, 67–76.
- [2] a) A. Quintas-Cardama, J. Cortes, *Clin. Adv. Hematol. Oncol.* **2006**, *4*, 365–374; b) J. F. Ohren, J. S. Sebolt-Leopold, *Nat. Chem. Biol.* **2006**, *2*, 63–64; c) F. J. Adrián, Q. Ding, T. Sim, A. Valentza, C. Sloan, Y. Liu, G. Zhang, W. Hur, S. Ding, P. Manley, J. Mestan, D. Fabbro, N. S. Gray, *Nat. Chem. Biol.* **2006**, *2*, 95–102; d) T. Asaki, Y. Sugiyama, T. Hamamoto, M. Higashioka, M. Umehara, H. Naito, T. Niwa, *Bioorg. Med. Chem. Lett.* **2006**, *16*, 1421–1425; e) C. M. McBride, P. A. Renhowe, T. G. Gesner, J. M. Jansen, J. Lin, S. Ma, Y. Zhou, C. M. Shafer, *Bioorg. Med. Chem. Lett.* **2006**, *16*, 3789–3792; f) E. Weisberg, P. Manley, J. Mestan, S. Cowan-Jacob, A. Ray, J. D. Griffin, *Br. J. Cancer* **2006**, *94*, 1765–1769.
- [3] a) F. Manetti, G. A. Locatelli, G. Maga, S. Schenone, M. Modugno, S. Forli, F. Corelli, M. Botta, *J. Med. Chem.* **2006**, *49*, 3278–3286; b) M. M. Schittenhelm, S. Shiraga, A. Schroeder, A. S. Corbin, D. Griffith, F. Y. Lee, C. Bokemeyer, M. W. Deininger, B. J. Druker, M. C. Heinrich, *Cancer Res.* **2006**, *66*, 473–481; c) G. Martinelli, S. Soverini, G. Rosti, M. Baccarani, *Leukemia* **2005**, *19*, 1872–1879; d) S. Kimura, H. Naito, H. Segawa, J. Kuroda, T. Yuasa, K. Sato, A. Yokota, Y. Kamitsuji, E. Kawata, E. Ashihara, Y. Nakaya, H. Naruoka, T. Wakayama, K. Nasu, T. Asaki, T. Niwa, K. Hirabayashi, T. Maekawa, *Blood* **2005**, *106*, 3948–3954; e) A. J. Tipping, S. Baluch, D. J. Barnes, D. R. Veach, B. M. Clarkson, W. G. Bornmann, F. X. Mahon, J. M. Goldman, J. V. Melo, *Leukemia* **2004**, *18*, 1352–1356; f) D. H. Boschelli, Y. D. Wang, S. Johnson, B. Wu, F. Ye, A. C. Barrios Sosa, J. M. Golas, F. Boschelli, *J. Med. Chem.* **2004**, *47*, 1599–1601; g) T. O'Hare, R. Pollock, E. P. Stoffregen, J. A. Keats, O. M. Abdullah, E. M. Moseson, V. M. Rivera, H. Tang, C. A. III, Metcalf, R. S. Bohacek, Y. Wang, R. Sundaramoorthi, W. C. Shakespeare, D. Dalgarno, T. Clackson, T. K. Sawyer, M. W. Deininger, B. J. Druker, *Blood* **2004**, *104*, 2532–2539.
- [4] F. Carraro, A. Naldini, A. Pucci, G. A. Locatelli, G. Maga, S. Schenone, O. Bruno, A. Ranise, F. Bondavalli, C. Brullo, P. Fossa, G. Menozzi, L. Mosti, M. Modugno, C. Tintori, F. Manetti, M. Botta, *J. Med. Chem.* **2006**, *49*, 1549–1561.
- [5] J. H. Hanke, J. P. Gardner, R. L. Dow, P. S. Changelian, W. H. Brissette, E. J. Weringer, B. A. Pollok, P. A. Connelly, *J. Biol. Chem.* **1996**, *271*, 695–701.
- [6] a) L. Tatton, G. M. Morley, R. Chopra, A. Khwaja, *J. Biol. Chem.* **2003**, *278*, 4847–4853; b) M. Warmuth, N. Simon, O. Mitina, R. Mathes, D. Fabbro, P. W. Manley, E. Buchdunger, K. Forster, I. Moarefi, M. Hallek, *Blood* **2003**, *101*, 664–672.
- [7] T. Chodhuri, S. Paul, M. L. Agwarwal, T. Das, G. Sa, *FEBS Lett.* **2002**, *512*, 334–340.
- [8] a) H. Yamaguchi, H. G. Wang, *J. Biol. Chem.* **2002**, *277*, 41604–41612; b) Y. T. Hsu, R. J. Youle, *J. Biol. Chem.* **1997**, *272*, 13829–13834; c) A. Letai, M. C. Bassik, L. D. Walensky, M. D. Sorcinelli, S. Weiler, S. J. Korsmeyer, *Cancer Cell* **2002**, *2*, 183–192; d) F. Gesbert, J. D. Griffin, *Blood* **2000**, *20*, 1179–1186.
- [9] T. W. Synold, I. Dussault, B. M. Forman, *Nat. Med.* **2001**, *7*, 584–590.
- [10] B. Nagar, W. G. Bornmann, P. Pellicena, T. Schindler, D. R. Veach, W. T. Miller, B. Clarkson, J. Kuriyan, *Cancer Res.* **2002**, *62*, 4236–4243.
- [11] G. Jones, P. Willett, R. C. Glen, *J. Mol. Biol.* **1995**, *245*, 43–53.
- [12] G. Jones, P. Willett, R. C. Glen, A. R. Leach, R. Taylor, *J. Mol. Biol.* **1997**, *267*, 727–748.
- [13] M. L. Verdonk, J. C. Cole, M. J. Hartshorn, C. W. Murray, R. D. Taylor, *Proteins* **2003**, *52*, 609–623.
- [14] D. Hudig, M. Djobadze, D. Redelman, J. Mendelsohn, *Cancer Res.* **1981**, *41*, 2803–2808.
- [15] M. Ogura, Y. Morishima, R. Ohno, Y. Kato, N. Hirabayashi, H. Nagura, H. Saito, *Blood* **1985**, *66*, 1384–1392.
- [16] K. Kishi, *Leuk. Res.* **1985**, *9*, 381–390.
- [17] F. Mohamadi, N. G. J. Richards, W. C. Guida, R. Liskamp, M. Lipton, C. Caufield, G. Chang, T. Hendrickson, W. C. Still, *J. Comput. Chem.* **1990**, *11*, 440–467.

Received: August 30, 2006

Published online on February 13, 2007